Article ID: 1003－6326(2003)02－0348－05

Microstructures of electromagnetic casting and direct chill casting LY12 aluminum alloys ①

CAO Zhi-qiang(曹志强), JIN Jun-ze(金俊泽), HAO Hai(郝 海), JIA Fei(贾 非)
(Research Center of Foundry Engineering, Dalian University of Technology, Dalian 116024, China)

Abstract: LY12 aluminum alloys made by electromagnetic casting (EMC) and direct chill casting (DCC), were analyzed by optical microscope, differential scanning calorimetry, transmission electron microscope and X-ray diffraction. It is found that the surface and subsurface quality of the ingot is improved largely due to the absence of an ingot mold, which is impossible to achieve with conventional DCC. It is also found that the intense forced convection can promote the fast superheat evacuation and break the dendrite arms, leading to the grain multiplication and the appearance of a fine equiaxed grains over the whole cross section. As a result, the hardness of EMC specimens increases one time than that from DCC in the as-cast state. Even though after the solid solution treatment and the artificial aging, the DCC ingot still can not get the same hardness as EMC ones.

Key words: electromagnetic casting; continuous casting; aluminum alloy; microstructure; hardness
CLC number: TG 249.7 **Document code:** A

1 INTRODUCTION

Electromagnetic casting (EMC) is a technology developed by the combination of magnetohydrodynamics (MHD) and casting engineering[1-3]. The EMC technology depends on the electromagnetic force to prevent the metal from touching the mold. Depending on the interaction of eddy currents induced in the metal and the magnetic field of the inductor, the liquid metal column is kept stable[4-6]. The contactless casting of EMC may eliminate the liquidation build-ups and feather crystals, relieve the scalping operation before the hot roll process, which is inevitable for direct chill casting[7, 8]. The more important merit is the fine and homogeneous grain size caused by the electromagnetic stirring in the melt. As a result, EMC has been paid great attention in China recently[5, 6]. Early researches concentrate more on the investigation of the electromagnetic formability and magnetohrodynamic phenomena of EMC technology[9-11], this paper aims mainly at the microstructures before and after heat treatment of EMC specimens.

2 EXPERIMENTAL

The LY12 aluminum alloy was cast by DCC and EMC techniques to contrast their microstructure and aging hardness; its nominal composition was Al-4.3Cu-1.6Mg-0.7Mn[12]. As a kind of widely applied hardening alloy, it is often used to fabricate the plane wrappings and aeroengine vanes working at high temperatures.

The experimental procedure was carried out on a pilot-scale caster, in which trial-and-error shaping experiments were performed and the optimized technical parameters have been obtained.

The basic apparatus of EMC consists of a delivery system, a casting control system, a shaping and a cooling system, a melting furnace and a power supply etc, as shown in Fig. 1. The magnetic field generated by a medium-frequency alternating current was used to pinch upon the molten aluminum[13] and a heavy eddy current was induced on the surface of the molten aluminum, which was in

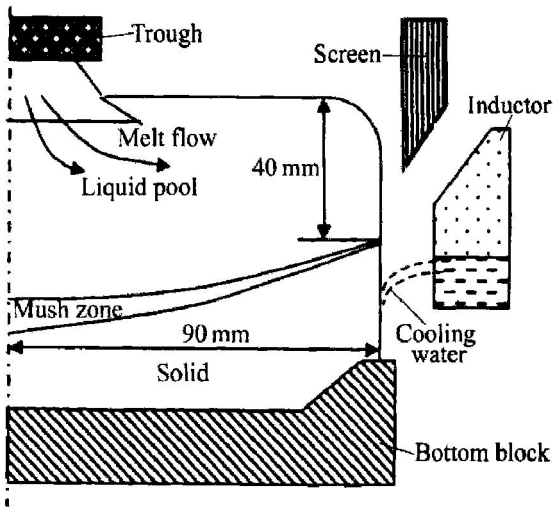

Fig. 1 Schematic illustration of EMC apparatus

① **Foundation item:** Projects (59901001, 59995442) supported by the National Natural Science Foundation of China; project (G1998061500) supported by the state key Fundamental Research and Development Program of China
Received date: 2002－04－16; **Accepted date:** 2002－07－05
Correspondence: Dr. CAO Zhi-qiang, Tel: +86-411-4706321; E-mail: caozq@dlut.edu.cn

opposite phase to the imposed current of the electromagnetic coil. By the way of the interaction of alternating magnetic field and induced current, a body force, directed towards the center of ingots, was generated to prevent the metal from touching the mold.

The technique procedures were as follows: firstly, the metal was melted; secondly, the position of inductor, screen, water jacket and bottom block were adjusted; thirdly, cooling system and power supply were turned on; at last the casting began in a withdrawal speed until the casting end. The manufacturing conditions were: inductor current 4 800A; height of liquid column 40mm; solidification front 10 mm up to bottom of inductor; pouring temperature 710 – 730 ℃; flow rate of cooling water 3 $m^3 \cdot h^{-1}$; casting speed 0.3 – 1.5 $mm \cdot s^{-1}$.

Besides the as-cast state, some LY12 specimens were solid solution-treated at 495 ℃ in salt bath furnace for 1 h and then quenched in ice water. After this, they were immediately aged in the 190 ℃ silicon oil bath for various holding period to obtain the hardening effect.

The metallographic specimens were prepared by cutting, grinding, polishing and etching. The etchant was Keller's solution. The specimens from DCC and EMC ingots were examined and contrasted by optical microstructure (OM) and X-ray diffraction (XRD).

Hardness tests were performed before and after heat-treatment by the load of 60 kg with the Rockwell hardness tester of F type. Take an average of 7 times after omitting the highest and the lowest values.

Differential scanning calorimetry (DSC) and transmission electron microscopy (TEM) were used to investigate the precipitation kinetics of aged specimens. The DSC specimens were heated to 530 ℃ from 30 ℃ at the rate of 10 $℃ \cdot min^{-1}$. The TEM specimens were prepared by twin-jet electro-polishing in 30% HNO_3-70 % CH_3OH (volume fraction) solution at – 30 ℃.

3 RESULTS AND DISCUSSION

Fig. 2 shows the transverse sectional microstructures of the LY12 DCC and EMC specimens in as-cast state. It is clear that the grains of EMC are much finer than DCC's, no matter at edge, midthickness or center of ingots. And in DCC condition, the grain size becomes coarse from the surface to the center of ingots. In contrast, the grain size decreases from the surface to the center of ingots due to the decrease of the cooling rate caused by the Joule heating at the subsurface zone of the ingot.

However, for the EMC, the grains are still homogeneous and fine than the DCC's over the entire cross section due to the strong electromagnetic stirring in the liquid pool[14-16]. This intense forced convection promotes a fast superheat evacuation and breaks the dendrite arms, which leads to the grain multiplication. The suspended nuclei localized in the vicinity of the liquid-solid interface are carried away and dispersed in a slightly super-heated melt. As a result, the crystallization takes place simultaneously in most of the sump and causes the appearance of a fine and uniform equiaxed structure over the entire cross-section[17-19].

XRD pattern in Fig. 3 shows that the main phases in EMC LY12 alloy are α, θ-$CuAl_2$ and S-$CuMgAl_2$. The principal strengthening phases are S'-$CuMgAl_2$, and θ′-$CuAl_2$[12]. Under the condition of non-equilibrium cooling during casting, elements copper and magnesium are retained in solid solutions, then, the super-saturated solid solutions (SSSS) are decomposed in the following sequence with increasing aging temperature:

$$SSSS \rightarrow \text{G. P. [I]} \rightarrow \text{G. P. [II]} \rightarrow S' \rightarrow S\ (CuMgAl_2)$$

$$SSSS \rightarrow \text{G. P. [I]} \rightarrow \text{G. P. [II]} \rightarrow \theta' \rightarrow \theta\ (CuAl_2)$$

Theoretically, as the G. P. [I] (solute-rich clusters) and G. P. [II] (vacancy-rich cluster) emerge, the strength of aluminum alloys increases. When the transition precipitation phase S' (θ′) comes up, the strength of aluminum alloys reaches the peaks at around 190 ℃. At last the equilibrium phase S (θ) turn up, and the mechanical properties begin drop[12, 13].

Fig. 4 shows the aging-hardening curves of LY12 alloys. It is found that the hardness of EMC specimens (HRF 31.7) is two times higher than that of DCC ones (HRF 16.0) due to the grain multiplication in as-cast state. The strength increases with the strengthening phase precipitation after the solution treatment. The EMC specimens reaches a peak (HRF 48.5) at around 12 h, while the DCC ones get the peak (HRF 44.4) at about 36 h after artificial aging. This means the EMC ingots have more obvious response to solution and aging treatment, compared to DCC ones.

The precipitation process of intermediate phases is shown in Fig. 5. The exothermic peaks at around 280 ℃ and 495 ℃ are respectively caused by G. P. [II] and S' (θ′) precipitates. No endothermic bump corresponding with the G. P. [I] zones emerges during the decomposing of alloys. The EMC specimens have higher exothermic precipitation peaks but narrow peak broadness than DCC ones.

Theoretically, the G. P. [I] zones are formed at a relatively low temperature and easier

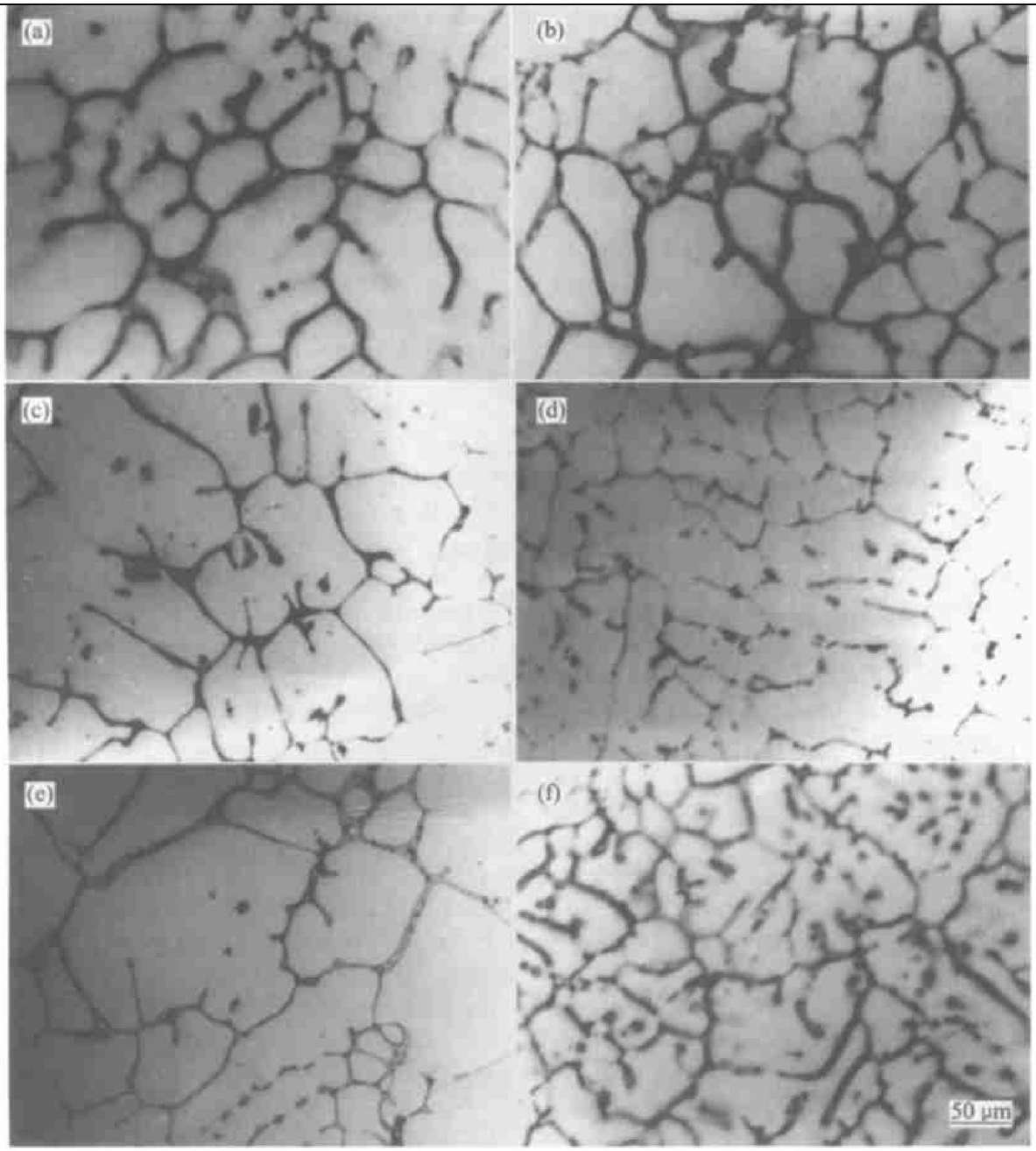

Fig. 2 Microstructures of LY12 alloy ingots (d 174 mm) at as-cast state
(a), (c), (e) —DCC, from surface to center; (b), (d), (f) —EMC, from surface to center

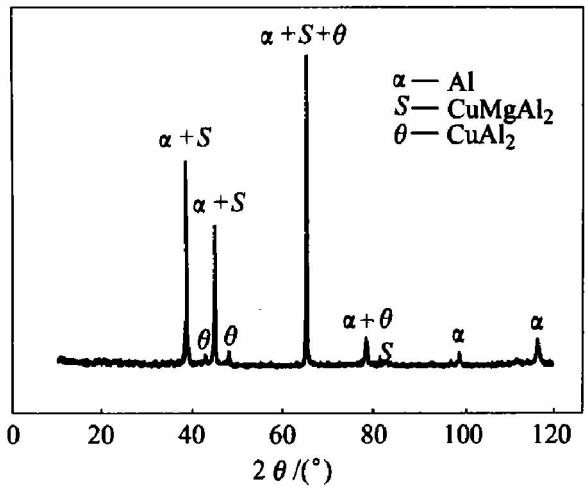

Fig. 3 XRD pattern on specimens of EMC LY12 alloys

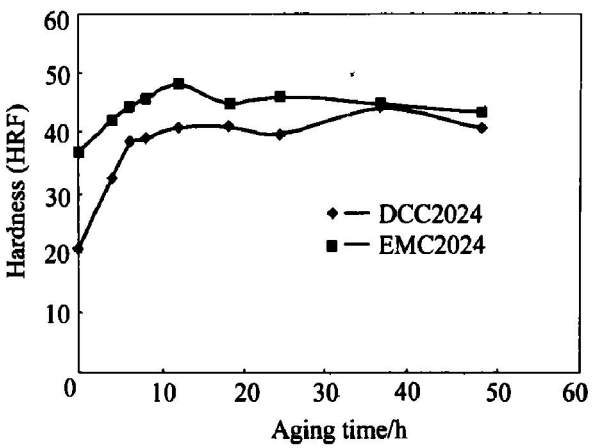

Fig. 4 Age-hardening curves of LY12 alloys

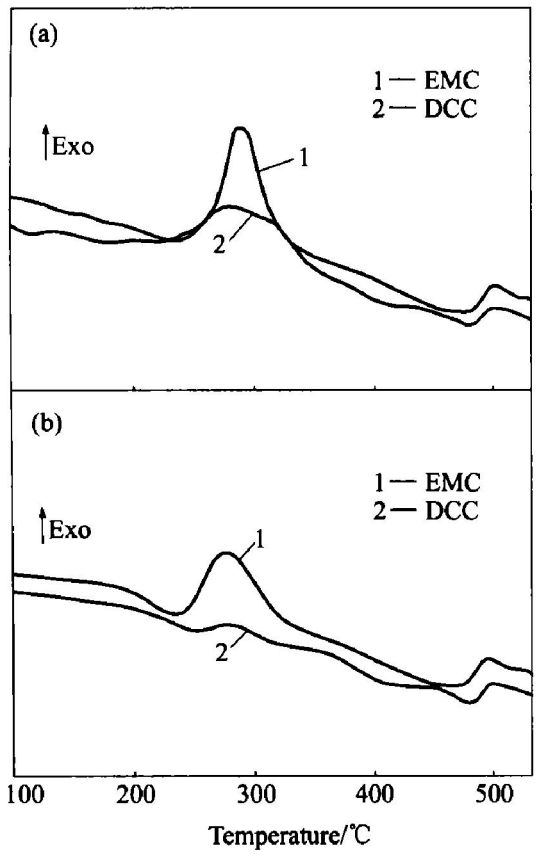

Fig. 5 DSC curves of LY12 alloys
(a) —As-quenched; (b) —As-aged

dissolved when the aging temperature rises[20]. As a result, the heat flow in aged state is lower than that in as-cast state. This can be explained by the fact that there is no coherent relationship between G. P. [Ⅰ] zones and matrix.

Fig. 6 shows that many rod and needle-like

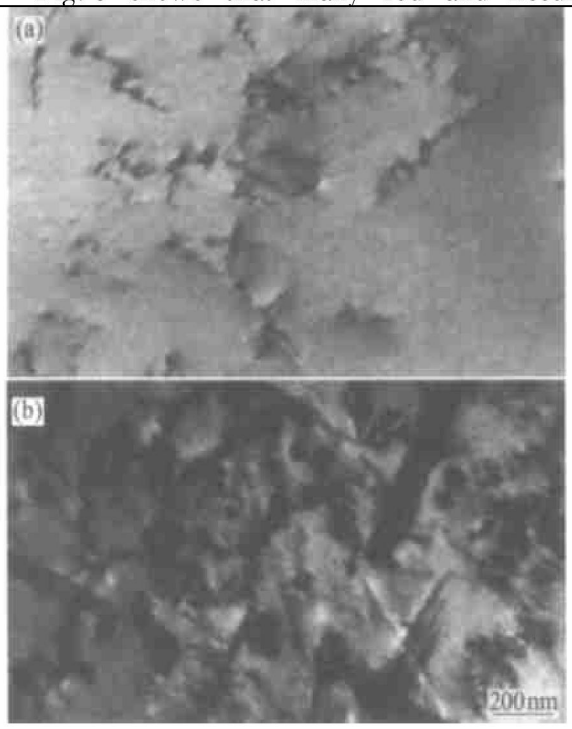

Fig. 6 TEM photographs of LY12 alloy samples at as-aged state
(a) —DCC; (b) —EMC

precipitates S' (θ') well distribute in EMC specimens and little in DCC specimens. It is suggested that fine equiaxed grains and short diffuse distance are beneficial to the fast precipitation of intermediate phases.

4 CONCLUSIONS

1) Electromagnetic stirring makes the EMC ingots have much fine grain sizes and homogeneous structures, and have higher hardness than DCC ones, not only in as-cast condition but also in as-aged state.

2) DSC results show that EMC specimens have higher enthalpy than DCC ones. This suggests that the G. P. zones and S' or θ' precipitation phases are more easily formed in EMC specimens than in DCC ones.

REFERENCES

[1] Getselev Z N. Casting in an electromagnetic field[J]. J Metals, 1971, 23(10): 38-39.

[2] Garnier M. Present and future prospect in electromagnetic processing materials[A]. Asai S. Proc International Symposium on Electromagnetic Processing of Materials [C]. Nagoya: ISIJ, 1994. 1-8.

[3] ZHANG Qin, LU Gui-min, CUI Jian-zhong, et al. Formation mechanism of non-dendritic structure of aluminum alloy produced by semi-continuous casting of CREM process[J]. Acta Metall Sinica, 2001, 37(8): 873-876.

[4] Prasso D C, Evans J W, Wilson I J. Heat treatment and solidification in the electromagnetic casing of aluminum alloys: part I. Experimental measurements on a pilot-scale caster[J]. Metall Trans B, 1995, 26B: 1243-1251.

[5] SHEN Jun, PEI Xin-feng, HOU Jian-ping, et al. Effect of coupling between melt shape and temperature field on electromagnetic shaping[J]. Trans Nonferrous Met Soc China, 2001, 11(1): 40-44.

[6] SHEN Jun, LI Jian-guo, FU Heng-zhi, et al. Analysis for electromagnetic pressure on thin platelike melt[J]. The Chinese Journal of Nonferrous Melts, 1999, 9(1): 173-177. (in Chinese)

[7] Sakane J, Li B Q, Evans J W. Mathematical modeling of meniscus profile and melt flow in electromagnetic caster [J]. Metall Trans B, 1988, 19B: 397-408.

[8] LIU Dan, CUI Jian-zhong, XIA Ke-nong. Non-dendritic structural 7075 aluminum alloy by liquidus cast and its semi-solid compression behavior[J]. Trans Nonferrous Met Soc China, 2000, 10(2): 192-195.

[9] Kageyama R, Evans J W. A mathematical model for the dynamic behavior of melts subjected to electromagnetic forces[J]. Metall Mater Trans, 1998, 29B(4): 919-928.

[10] XING Shu-ming, ZENG Da-ben, HU Han-qi, et al. Prediction of remained shell dimension of semisolid continuous casting process[J]. The Chinese Journal of Nonferrous Melts, 2000, 10(6): 800-803. (in Chinese)

[11] Vives C. Effects of a magnetically forced convection during the crystallization in mould of aluminum alloys [J]. J Crystal Growth, 1989, 94(3): 739-750.

[12] Mondolfo L F. Aluminum Alloys: Structure and Prop-

erties[M]. London: Butterworths, 1976. 693.
[13] Furui M, Kojima Y, Matsuo M. Fabrication of small aluminum ingot by electromagnetic casting[J]. ISIJ International, 1993, 33(3): 400－404.
[14] Higgins R A. The Properties of Engineering Materials [M]. London: Edward Arnold, 1994, 264.
[15] ZHANG Kui, LIU Guo-jun, XU Jun, et al. Semi-solid Al-7% Si alloy prepared by electromagnetic stirring-continuous casting technology and its solidification microstructures[J]. The Chinese Journal of Nonferrous Melts, 2000, 10(1): 47－50. (in Chinese)
[16] Kamado S, Kosaka T, Kabayama Y, et al. Fabrication of 5052 aluminum alloy thin slab by electromagnetic casting and mechanical properties of its cold-rolled sheet [J]. Materials Science Forum, 1999, 327(4): 473－478.
[17] ZHANG Kui, LIU Guo-jun, ZHANG Jing-xin, et al. Application of semi-solid Al alloys processing [J]. The Chinese Journal of Nonferrous Melts, 2000, 10(Suppl. 1): 135－140. (in Chinese)
[18] ZHANG Jing-xin, ZHANG Kui, LIU Guo-jun, et al. Formation mechanism of non-dendritic structure in semi-solid metals produced by ES process[J]. The Chinese Journal of Nonferrous Melts, 2000, 10(4): 511－515. (in Chinese)
[19] Asai S. Birth and recent actions of electromagnetic processing of materials[J]. ISIJ International, 1989, 29 (12): 981－992.
[20] Yuan S Y, Yeh J W, Tsau C H. Improved microstructures and mechanical properties of LY12 aluminum alloy produced by a reciprocating extrusion method[J]. Mater Trans JIM, 1999, 40(3): 233－241.

(Edited by LONG Huai-zhong)